Eigenstrain modelling of residual stress generated by arrays of Laser Shock Peeing shots and determination of the complete stress field using limited strain measurements

M. Achintha, D. Nowell, K. Shapiro, P.J. Withers

PII: S0257-8972(12)01172-3
DOI: doi: 10.1016/j.surfcoat.2012.11.027
Reference: SCT 18201

To appear in: *Surface & Coatings Technology*

Received date: 9 June 2012
Accepted date: 8 November 2012

Please cite this article as: M. Achintha, D. Nowell, K. Shapiro, P.J. Withers, Eigenstrain modelling of residual stress generated by arrays of Laser Shock Peeing shots and determination of the complete stress field using limited strain measurements, *Surface & Coatings Technology* (2012), doi: 10.1016/j.surfcoat.2012.11.027

Eigenstrain modelling of residual stress generated by arrays of Laser Shock Peeing shots and determination of the complete stress field using limited strain measurements

M. Achintha[a*], D. Nowell[b], K. Shapiro[c], P. J. Withers[c]

[a] Faculty of Engineering and Environment, University of Southampton, Southampton, SO17 1BJ, UK

[b] Dept. of Engineering Science, University of Oxford, Parks Road, Oxford, OX1 3PJ, UK

[c] School of Materials, University of Manchester, Grosvenor Street, Manchester, M17HS, UK

* Corresponding author: e-mail: Mithila.Achintha@soton.ac.uk Tel: +44(0)7500197739

Abstract

This paper presents a hybrid explicit finite element (FE) /eigenstrain model for predicting the residual stress generated by arrays of adjacent/overlapping laser shock peening (LSP) shots where the use of a completely explicit FE analysis may be impractical. It shows that for a given material, the underlying eigenstrain distribution (in contrast to the resulting stress field) representing a laser shock peen is primarily dependent on the parameters of the laser pulse and the number of overlays rather than the precise component geometry. Consequently the residual stress introduced by complex laser peening treatments can be built up by using static FE models and superposition of individual eigenstrain distributions without recourse to further computationally demanding explicit FE analyses. It is found that beneath a small patch of LSP array the magnitude of the compressive residual stress is higher than for a wider array of LSP shots and that with increasing numbers of layers the compressive stress increases as does the depth of the compressive zone. The model predictions for the eigenstrain distributions are compared well with experimental measurements of plastic strain (full-width-at-half-maximum) obtained by neutron diffraction. The eigenstrain method is also extended

to construct the full residual stress field using measured residual elastic strains at a finite number of measurement locations in a component.

***Keywords*:** Eigenstrain, Laser shock peening, Plastic strain, Residual stress

1. Introduction

The authors have previously [1] developed a hybrid explicit finite element (FE) / eigenstrain (i.e. misfit strain) model to determine the residual stresses generated by a single laser shock peening shot (LSP). This paper extends the hybrid eigenstrain model to characterise the residual stress generated by arrays of adjacent and/or overlapping shots, representing practical LSP applications (e.g. surface treatment at the root of a fan blades of aircrafts engines [2]).

Laser shock peening uses high intensity laser pulses to generate a compressive residual surface stress in critical metal structural components. The technique is used to improve the structural performance of highly-stressed components used in aircrafts (e.g. fan blades of engines). It can also be used as a part of a forming process (e.g. in wing panels). Usually the surface area to be treated is covered by a sacrificial aluminium tape prior to the laser shock treatment. The laser beam produces locally a rapidly-expanding plasma (due to the vaporisation of the aluminium tape) which is confined by a jet of water simultaneously sprayed on the surface. This confinement of the plasma generates a high-amplitude, short duration shock (pressure) wave and the sacrificial layer ensures that there is no significant heating in the substrate [1, 3]. The stresses generated in the workpiece due to the propagation of the stress wave cause plastic deformations in the surface region of the material and, once the pulse has decayed, the misfit between the plastically deformed material and surrounding undeformed bulk generates a residual stress field [1]. Typically, LSP produces surface compressive stress to a depth of 1-2 mm, which is about five to ten times deeper than that produced by conventional shot peening [1, 3]. A significant advantage of LSP is that the laser parameters can be controlled more precisely and repeatably than their equivalents in shot peening, and this allows the process to be tailored to specific design requirements.

Although the LSP technique has significant potential to improve the fatigue resistance of highly-stressed components, the lack of practical predictive tools means that the technique has not been used effectively as it might be. In particular, unless great care is taken the balancing tensile stresses [1] may actually reduce fatigue life, and hence knowledge of the locations and magnitudes of these tensile stresses is required. However, these can be difficult to determine because the residual stress arises as the result of the elastic response of the whole component to the plastic strain introduced by LSP. The effects of LSP in complex geometries (e.g. along the leading edge of a fan blade) and where stress concentrations are present (and hence where the treatment is most useful) can be even more difficult to predict. The hybrid eigenstrain-based FE model developed by the authors [1] uses an explicit (i.e. dynamic) FE simulation of the shock wave caused by a laser pulse, which allows characterisation of the eigenstrain introduced by the process. The residual stress can then be determined by installing the eigenstrain distribution in a static FE model. The model is more physical than simply modelling residual stress in the sense that it captures the misfit strain, to which the residual stress is a response. The method also reduces the computational cost significantly since a wholly explicit FE analysis must be run until the stress waves dissipate fully.

Since the sacrificial aluminium tape ensures that, over the short duration of the pulse (usually < 30 ns), no significant heating occurs in the workpiece, the generation of the residual stress field due to LSP may regarded as a mechanical process [1]. The present model relies on identifying the eigenstrain (plastic strain) needed to represent the residual stress state predicted by the explicit FE model. Eigenstrains act as sources of incompatibility of displacement and provide a powerful technique for the representation of residual stress states [4]. Any residual stress state can be represented as a distribution of eigenstrain over a suitable volume, either in a FE model or using an analytical approach. The technique has been successfully used to predict residual stresses generated in various applications. For instance,

Korsunsky et al. [5] successfully constructed the residual stress induced by welding; Prime and Hill [6] determined fibre scale residual stress variation in metal-matrix composites; and Korsunsky [7] evaluated residual stresses in autofrettaged tubes. A similar approach has been used by DeWald and Hill [8] to determine the residual stress generated by LSP.

Once the eigenstrain distribution has been determined for the chosen laser setting, the residual stress field can be determined by simply installing the eigenstrain in an appropriate static FE model. The use of eigenstrain analysis to model the LSP process has a number of advantages. We have earlier shown that the plastic strain caused by the shock wave has usually stabilised within 1–2 μs after the pulse [1], after which the underlying eigenstrain can be extracted from this analysis. The residual stress can then be obtained from a single subsequent static FE simulation. We shall also show that the eigenstrain repressing a given laser peen is largely unaffected by the component geometry or the sequence and arrangement of neighbouring peens. Thus, once the eigenstrain has been computed using simple analyses the residual stress introduced in new geometries and/or during subsequent loading can be calculated in a computationally efficient manner, simply by imposing the accumulated eigenstrain on the appropriate static FE models. Formulation of the solution this way ensures global stress equilibrium, strain compatibility, and also matches the boundary conditions. The step-by-step procedure of the present hybrid model is shown in Fig. 1. We have earlier [1] shown that the results from this eigenstrain-based analysis agree well with those obtained from the stabilised solution of an equivalent wholly explicit FE simulation.

In practice even with high power laser sources, commercial LSP providers can only peen a region of a few square millimetres in a single pulse [9]. This means that a large number of LSP pulses placed side by side are required to treat a surface region. In an array of LSP pulses, the individual shots are typically arranged with an overlap of about 5–10% of the

width of a pulse between the adjacent shots [9]. In practice, it is also common to apply more than one layer of shots, since this produces a deeper layer of compressive stress. A completely explicit FE simulation of an array of pulses would therefore require explicit modelling of a large number of shots. Consequently, a wholly explicit FE analysis of a practical array of LSP shots would be computationally impractical. This paper examines the degree to which complex peening strategies can be modelled by simple eigenstrain distributions and the results show that the effect of multiple shots can be rapidly assessed by superposition of eigenstrains.

A further application of the eigenstrain method may also be explored. In an experiment, the residual stresses cannot be measured directly; rather they are deduced from measured residual elastic strains (e.g. by using neutron diffraction tests) using a suitable form of Hooke's law. Because of practical difficulties, residual strains are usually only measured at a finite number of measurement locations within a specimen. Consequently, determination of the full residual stress field (i.e. six continuously varying components of stress that satisfy equilibrium, compatibility and the boundary conditions) from these test data is an extremely challenging problem, particularly in the presence of experimental error or uncertainty. In this paper we extend the eigenstrain methodology to infer the full residual stress field in a specimen based on a finite number of measurements. This is achieved by determining a representative eigenstrain distribution for a given sample (e.g. by matching the test data in a least squares sense). This may then be used to predict the residual stress state in the whole specimen in a way that is consistent with the underlying requirements of equilibrium and compatibility.

2. Modelling approach

The approach previously [1] used in the process modelling of a single LSP shot is extended here in order to determine the residual stress generated by multiple shots. As an example we will discuss the analysis of a 20 mm x 25 mm x 12 mm Ti-6Al-4V block, peened by an

rectangular array of twenty LSP shots (each 3 mm x 3 mm; laser power density I = 9 GW/cm^2; pulse duration t_L = 18 ns; energy efficiency of the process η = 4.5%). The efficiency factor of the LSP process, η, is defined based on the supplied laser energy, and the energy transferred to the workpiece and this analysis is described elsewhere [1]. Ti-6Al-4V was chosen in the current study because of its widespread use in the aerospace industry. An 4 x 5 (x direction by y direction) array of LSP shots is applied to the central region of one of the large faces so that it covers 36% of total surface area (Fig. 2). For simplicity, it is assumed that there is no overlap between adjacent pulses. In order to facilitate understanding of the approach, a brief overview of the analysis of a single pulse is given below.

2.1 Eigenstrain modelling of a single LSP shot

An explicit FE simulation of the laser-induced shock wave is first carried out in order to determine the eigenstrain distribution.

2.1.1 Modelling of the LSP loading

The explicit FE simulation requires the spatial distribution and time history of the pressure load representing the laser pulse. Both quantities are difficult to determine directly, analytically or experimentally, but a method has been developed by the authors [1] to estimate the peak pressure and the duration of the pressure load to an acceptable accuracy by considering the energy transmitted to the workpiece during LSP. It is assumed that the pressure front develops uniformly over the area covered by the laser pulse (A_L). Although a drop in pressure might be expected towards the edges of the pulse, experimental evidence shows an approximately uniform surface indent in the workpiece following a single LSP pulse (an example is shown in Fig. 3a). This suggests that edge effects are not significant and the assumption of a uniform pressure front in the modelling is acceptable. Also it is important

to appreciate in practice LSP shots are overlapped by a small amount in order to counteract any edge effects.

As regard the temporal variation in the pressure pulse; since our current study is focused on characterising the basic mechanics of the LSP process, it is convenient to assume a simplified pressure/time (p–t) variation. A triangular ramp with the peak pressure (p_{max}) occurring at the half the total pulse duration (t_p) was therefore assumed (Fig. 3b). Thus, the p–t relationship can be described using only two parameters: p_{max} and t_p. Values which are broadly representative of peening conditions are determined so that they are consistent with the input laser energy and a representative energy efficiency. Details of this analysis are presented elsewhere [1]; a typical pulse of a used commercial laser system (I=9 GW/cm^2, t_L=18 ns and η=4.5 %) is reasonably well represented by a dynamic pressure load with p_{max} = 6.7 GPa and t_p = 100 ns.

2.1.2 Material model for Ti-6Al-4V

The results of earlier LSP analyses for Ti-6Al-4V [1] suggest that the material will experience strain rates of the order of 10^6 s^{-1}. In such circumstances, relatively sophisticated material models such as the Johnson–Cook model [10], which incorporates strain and strain rate hardening, may appear to give a more appropriate representation of material behaviour. However, in practice the material parameters required are very difficult to determine. As a result the complexity of the material model can simply obscure the underlying physical behaviour. It should also be noted that the Johnson–Cook model frequently only calibrated against test data for strain rates up to 10^4 s^{-1}, hence extrapolating the model to strain rates of the order of 10^6 s^{-1} will give an additional source of uncertainty. Since our study is focused primarily on the basic mechanics of the LSP process it is appropriate to employ a simple model so as to keep the number of material parameters to a minimum. We have therefore

assumed elastic/perfectly-plastic behaviour with parameters broadly representative of Ti-6Al-4V (yield stress (σ_y) 1000 MPa; Young's modulus (E) 110 GPa; Poisson's ratio (υ) 0.3; and density (ρ) 4400 kg/m^3). This simplified model effectively represents a generic material behaviour and with suitable scaling, may be considered as representative of a range of engineering alloys.

2.1.3 Extraction and representation of the eigenstrain distribution

Once the explicit FE analysis has been run (LS-DYNA [11] is used in the present study), it is necessary to extract the eigenstrain distribution. This can be done once the plastic strains are stabilised (usually after a period of 10–12 times the pulse duration, t_p (i.e. ~1–2 μs)) [1]. Plastic deformation will always cease at some time after the pulse, and the remaining deformation (basically a 'ring down') will be elastic. The stabilised plastic strain state may be conveniently determined by using the time-history plots of the plastic strain in the results of the explicit FE simulation and this analysis is presented elsewhere [1]. Fig. 4a shows the results obtained from the explicit FE model for the stabilised plastic strain for a typical specimen after a single LSP shot. The variation of eigenstrain across the width of a single LSP shot at two different depths (at z= 0 and z=1.0 mm respectively) is shown in Fig. 4b (symmetry consideration means only a half of the width is shown here). As described previously (Section 2.1.1), the experimental evidence (Fig. 3a) shows mostly a uniform surface indent under a LSP shot and this agrees well with the model results. However, it should be noted that although a relatively low eigenstrain is expected due to the expected drop in pressure towards the edge, Fig 4b shows a contradictory result that a relatively high eigenstrain at the surface (z= 0 mm) in the vicinity of the edge of the pulse. This is an artefact of the spatial pressure distribution used in the analysis where a step change to zero was assumed at the edges. This is unlikely to be precisely the case in practice. Nevertheless, Figs. 4a and 4b show that, neglecting edge effects, the distribution is approximately uniform with x

and *y*, over the whole area subjected to the pulse. It is therefore an appropriate simplification to represent the misfit by an eigenstrain that varies only with depth (*z*). Fig. 4c shows the variation of one of the in-plane eigenstrain components (ε_{xx}^{p}) with z. The approximately constant value of eigenstrain within ~1.1 mm of the surface is due to the reverse plastic flow caused by the unloading phase of the dynamic pressure load [1]. In order to conveniently incorporate the eigenstrain as a misfit strain, it is useful to represent the variation with *z* approximately as a polynomial function of *z* (shown in solid line in Fig. 4c). It was determined that the variation of eigenstrain with *z* can be conveniently approximated by two fourth order polynomials; the approximately constant eigenstrain zone (i.e. $0<z<1.1$ mm; coefficients of the polynomial 0.00142362, -0.00193614, -0.00011240, 0.00087460, 0.00602791) and the zone where the eigenstrain gradually decreases (i.e. $1.1 \text{ mm}<z<2.3$ mm; coefficients of the polynomial 0.00438734, -0.03122438, 0.08275209, -0.10120292, 0.05230886). The residual stress distribution is then obtained by incorporating three principal components of eigenstrain ($\varepsilon_{xx}^{p}, \varepsilon_{yy}^{p}$ and ε_{zz}^{p} respectively) in an appropriate elastic-static FE model (ABAQUS/Standard [12] is used in the present study). This is achieved by specifying anisotropic thermal expansion coefficients that vary with position, together with a uniform (unit) temperature rise [1]. This has the effect of introducing the correct eigenstrain at each point in the workpiece.

3. Analysis of a single layer of adjacent LSP shots

To illustrate the effect of an array of shots, we will analyse the same Ti-6Al-4V specimen described above (20 mm x 25 mm x 12 mm), peened by a rectangular array of twenty LSP shots (each 3 mm x 3 mm) (Fig. 2). In order to determine the eigenstrain caused by the complete array of LSP shots, an explicit FE simulation was first carried out. This was conveniently achieved by applying representative dynamic pressure loads (p_{max}= 6.7 GPa and t_p=100 ns), representing each LSP shot at appropriate time intervals. The time interval

between subsequent shots was determined by the need to allow the response to the previous pulse to have stabilised. This was achieved by turning on material damping after each shot (once the initial plastic deformation was complete) and turning it off before applying the subsequent shot. It was found that the residual stress field stabilised about 20-25 ms after the start of the LSP pulse. This time interval is significantly shorter than the repetition rate that the subsequent shots are pulsed in commercial LSP applications (≈ 2-10 pulses/second) [9].

Figure 5a shows the results obtained from the explicit FE simulation for the distribution of stabilised plastic strain in the specimen after the application of all the LSP shots. From the figure it is evident that, neglecting edge effects (i.e. in the vicinity of edges of each individual pulse), the distribution of eigenstrain is largely uniform with *x* and *y*, over the whole area subjected to LSP. It is therefore appropriate to assume that the eigenstrain varies only with depth (*z*). It should be noted that the results of explicit FE simulations (Fig. 5a) show that stress waves develop at the corners of each LSP pulse propagate approximately in the diagonal direction towards the centre of the adjacent shots. Unfortunately, because of the chosen contour scale in Fig. 4a, this minor non uniformity is not visible whereas the chosen different contour scale in Fig. 5a shows a small non uniformity of plastic strain at the centre of individual LSP pulses. Fig. 5b shows the variation of one of the in-plane eigenstrain components (ε_{xx}^{p}) with *z* at three different locations, corresponding to different rows of the array (Locations A, B and C in Fig. 5a). The results show that the variation of ε_{xx}^{p} with *z* is approximately the same at various locations within the array and it is noteworthy that it is almost identical to that generated by a single LSP shot (Fig. 4c). Similar observations can be made about the other eigenstrain components (ε_{yy}^{p} and ε_{zz}^{p}). This result suggests that the eigenstrain caused by each pulse in an array develops directly under the area covered by the respective shot and is not significantly influenced by the pre-existing residual stress and eigenstrain states present in the surrounding area. The distribution of eigenstrain is also

mostly unaffected by the order in which the pulses were applied. Therefore, it is appropriate to model the eigenstrain caused by the array of shots as having the same variation with *z* as that generated by a single shot (Fig. 4c) but applied over a wider (*x*, *y*) area. The residual stress field in the specimen can then be determined simply by introducing the eigenstrain depth profile shown in Fig. 4c over the required area in the static FE model, thereby massively reducing the computational cost compared to an explicit FE simulation of each LSP shot.

The in-plane residual stress component (σ_{yy}), obtained by incorporating the eigenstrain distribution shown in Fig. 4c is shown in Fig. 6a. As expected, a compressive stress layer is developed directly under the area covered by the array (within $z < 1.75$ mm), with counter-balancing tensile stresses beneath. The figure shows that the variation of σ_{yy} is approximately uniform in *x* and *y* directions over the area covered by the LSP shots. The profile of the results agree well with those measured experimentally such as the study of Masse and Barreau [13] who looked at LSP of hypereutectoid steel specimens. It should be noted, however, that the edge effects will depend on how the eigenstrain distribution is terminated at the edges of the array. Here a step change to zero is assumed at the edges and this is unlikely to be precisely the case in practice. Fig. 6b shows the variation of σ_{xx} and σ_{yy} with *z* at the centre of the array (σ_{xx} and σ_{yy} are not identical here because of the rectangular geometry of the specimen and the patch). It is evident from the σ_{xx} and σ_{yy} stress components close to the surface (-490 MPa and -560 MPa respectively) that the stress developed is slightly higher in the direction of the longer dimension of the array (5 shots) compared to that in the shorter dimension (4 shots). The magnitude of the compressive stress increases slightly with depth up to 1.1 mm deep. It is also noteworthy that peak tension (300 and 270 MPa for σ_{xx} and σ_{yy} respectively) occurs approximately at the depth where the eigenstrain falls to zero ($\approx$ 2.3 mm).

The solid line in Fig. 6b shows the distribution of σ_{yy} with z at the centre of the peened area if the specimen was peened by a single pulse (3x3 mm) using the same laser parameters. It is clear from Fig. 6b that a single pulse produces a similar surface stress to that for the array. However, here the compressive plateau with increasing depth is not as marked. Since the eigenstrains are similar, comparison of these results highlights the effect of the constraint provided by the surrounding material on the stress field developed, in particular the subsurface tensile peak is only 190 MPa compared to 270 MPa for the array. This is because when the surface is treated by an extended patch of LSP pulses, the requirement for through-thickness equilibrium of forces and moments in the specimen becomes significant whereas for a single shot, a part of counterbalancing tensile stress develops outside of the area covered by the pulse [1].

4. Analysis of multiple layers of LSP shots

In practice it is common to apply one or two further layers of LSP shots on the top of the initial layer (referred to as a 200% or 300% peen respectively), in order to achieve a deeper compressive residual stress. Subsequent layers are normally applied so that the individual shots are 50% offset relative to those of the previous layer in both *x* and *y* (Fig. 7a) [9].

4.1 Two layers of peening

As an example, the analysis of two layers of shots will be discussed, using the same geometry and the same laser setting considered above with 50% offset. As before, for simplicity, no overlap was assumed between the shots within the same layer. Given that we found that the eigenstrain caused by an array of shots to be similar to that of a single shot, we can study the eigenstrain introduced by 50% overlap double peening by analysing initially a simple array comprising four adjacent shots forming a square patch with a fifth shot applied centrally on top of the first layer (Fig. 7b).

An explicit FE simulation of the simple five pulse array (Fig. 7b) was first run to determine the eigenstrain distribution as shown in Fig. 7c. It is evident that the distribution of eigenstrain in the area covered by the second layer is also approximately uniform in the *x* and *y* and that the eigenstrain in the rest of the specimen is essentially unaffected. Thus, it is appropriate to model the eigenstrain caused by two layers of shots as a uniform distribution (in the *x* and *y* directions) equal to that found in the 200% peen region. Fig. 8 shows the variation of one of the in-plane components of eigenstrain (ε_{yy}^{p}) with *z*, generated by one and two layers of LSP shots. In both cases the variation in ε_{yy}^{p} is approximately constant to a depth of 1.1. mm, but the magnitude of eigenstrain is much greater for two layers (~ 50% larger) and extends deeper below the surface (3.2 mm compared to 2.3 mm for single layer) . In conclusion, the residual stress caused by the two layers of LSP can be determined using the eigenstrain distribution shown in Fig. 8; the results will be discussed in Section 5.

4.2 Three layers of LSP shots

The results in the previous section have shown that the eigenstrain distribution introduced by each LSP pulse in an array is limited to the area covered by the respective shot. This has the advantage that the eigenstrain arising from each 100% or 200% peen can be determined without having to take into account all other LSP pulses, thereby substantially simplifying the analysis. Following the same argument the eigenstrain distribution caused by a 300% peen can be established by explicitly modelling a small array of shots. Fig. 9a shows the appropriate array of three LSP shots, where the second and third shots were arranged to give 50% overlap with the first shot in the *x* and *y* directions respectively. Fig. 9b shows the eigenstrain distribution (determined from an explicit FE simulation) at the surface of the specimen after each LSP shot. As expected, the results show that the eigenstrain distribution is uniform with *x* and *y* in each of the three types of areas (100%, 200% and 300% peen).

The eigenstrain variations with depth for the 200% and 300% treated areas are compared (Fig. 10) with that for the doubly peened areas considered earlier in Fig. 7. As one might expect the result for the 200% peened area is essentially the same as that for the previous 200% peen case, despite the smaller doubly peened area considered here. Thus, it can be concluded that the eigenstrains are not substantially influenced by the actual area of the array, and a representative distribution may be determined from an explicit FE simulation of a simplified configuration. The third layer introduces an additional near surface eigenstrain (approximately 30% of that caused by the first pulse) and also extends the depth of the affected zone (to about 3.8 mm). It will be noted that the additional eigenstrain caused by the third layer of shots is less than that caused by the second. This decrease in the additional eigenstrain introduced with each successive layer is due to the pre-existing residual stress state, which acts to inhibit further yield of the material. With a work-hardening material this effect will be even marked, although it should be noted that Ti-6Al-4V shows very low levels of work hardening [14] and the material model assumed here is probably appropriate.

4.3 Effect of the degree of overlap between the subsequent layers

The results in the previous section show that the eigenstrain introduced by LSP is mostly independent of the area treated. These results suggest that the eigenstrains are not significantly affected by the overlap pattern used between the pulses in subsequent layers of LSP shots. To examine this further, Fig. 10 compares the eigenstrain obtained from explicit FE modelling of layers generated by shots with 50% offset and with 0% offset (i.e. where the shots of each layer precisely coincide with those below). It can be seen (Fig. 10) that the eigenstrain distributions are essentially the same and it can be concluded that the eigenstrain generated in a specimen depends only on the number of LSP layers applied and not on the precise arrangement of the shots in each layer. However, it should be noted that we have not

chosen to examine the question of edge effects, since we cannot be confident that our assumption about the spatial pressure distribution at the edge of each pulse is correct. In any case, it is likely that because overlaid pulses are offset in practice this will minimise significance of edge effects due to individual shots.

4.4 Experimental validation of the eigenstrain predictions

In an earlier paper by two of the present authors [1], the eigenstrain modelling of single LSP shots were validated against the experimental measurements of surface deformation. Further validation can be obtained by comparing the model predictions for eigenstrains with estimates of plastic strain distribution obtained by the angular shift in the peak position of the diffracted beam (expressed as full-width-at-half-maximum–FWHM). Neutron diffraction [15] was used to determine the residual strain (the angular shift in the peak position of the beam) and the extent of plasticity (FWHM measurements). FWHM values provide a measure of the local distribution of crystallographic orientation and hence may be taken as an indication of the plastic strain present in the specimen [16]. Thus, one might expect that high FWHM values in areas of high plastic strain (and hence high eigenstrain), although a direct quantitative relationship between the two parameters is more difficult to establish. In particular, it should be noted that if the plastic strain is reversed (as occurs during passage of the unloading stress wave during LSP), the eigenstrain will reduce [1], but the FWHM value is likely to increase. Nevertheless, FWHM measurements can provide a useful validation of the eigenstrain modelling approach as outlined below.

Point by point diffraction [1011] peak measurements were made on the SALSA diffractometer at the ILL, Grenoble through the depth of the peened samples using a 10 mm x 0.8 mm x 0.8 mm at 44.82° scattering angle using neutrons of wavelength 1.7Å. Fig. 11a shows the variation of measured FWHM with z at the centre of the peened area for a specimen

peened by an array of two layers (each with pulses of I = 9 GW/cm^2). The results show a plateau indicative of constant plastic work till a depth of 1.2 mm followed by a fall to the background value at 3.3 mm or so (Fig. 11a). A qualitative comparison between the FWHM values and the eigenstrain predicted by the model is shown in Fig. 11b for three different 200% peen conditions (I = 3, 6 and 9 GW/cm^2 respectively). To facilitate the comparison, the background level of FWHM has been subtracted to give ΔFWHM and this is plotted with the predicted eigenstrain against a single axis (since fortuitously the two quantities have very similar values in the units used). The figure shows that, for all laser settings, the variation of ΔFWHM with z is similar to that of eigenstrain. Furthermore, the depth of the plastically deformed zone matches the predicted eigenstrain depth. Although it is difficult to directly relate the magnitude of ΔFWHM to that of eigenstrain, it is expected that there must be a consistent relationship between the two quantities for the whole range of eigenstrain values, and that this relationship should be independent of the laser power. Fig. 11c plots the two quantities directly against each other and shows that, neglecting the region where reverse plasticity [1] has taken place (i.e. up to 1.3 mm below the surface), there is an approximately linear relationship.

5. Residual stress distribution

In a previous study we undertook a parametric study of the effect of different laser intensities on the residual stress distribution generated by single LSP shots [1]. Here we will investigate the effects of multiple layers of LSP shots both as a 4 x 5 array and a 1 x 1 array (single 100% overlapping shots) all peened using I = 9 GW/cm^2 (p_{max}=6.7 GPa and T_p=100 ns). The residual stress field generated by each peening set-up was determined by applying the polynomial form of the eigenstrain distribution at the correct locations within appropriate static FE models.

Figure 12 compares the variation of one of the in-plane residual stress components, σ_{yy}, with *z*, at the centre of the peened area for all six cases described above. Considering initially the single spots, it is clear that moving from a single peen to a double, or triple, peen increases the surface compressive stress from 550 MPa to 830 and 1120 MPa respectively; the depth of compressive layer increases from 1.8 mm to 2.4 mm and 2.7 mm. The magnitude of the counterbalancing tension does not change significantly but the peak tension moves from a depth of 2.3 mm to 3.4 and 3.7 respectively (this location coincides approximately with end of the applied eigenstrain distribution in each case). The corresponding peened arrays all show higher balancing tension (270, 360, 430 MPa respectively) than the single shots, although the location is approximately the same. For the arrays, the increase in the magnitude of the compressive plateau due to the application of multiple layers (560, 610 and 780 MPa respectively for 100%, 200% and 300% peen) is less marked than that for single shots. However, the depth of the compressive layer appears largely unaffected by the peened area. It should be remembered that the depth profile of the eigenstrain for the single spots and the arrays are identical (for a given set of peening parameters), but the different area treated affects the generated residual stress. This reflects the different amount of elastic constraint provided by the surrounding elastic material. The residual stress arises as the result of the elastic response of the component to the plastic strain introduced by the LSP. For a small peened area, some of the balancing tension is carried by the outside unpeened area, which is not the case at the centre of a large array. This underlines the applicability of the eigenstrain method: the eigenstrain distribution can be viewed as a response to the LSP and it is largely independent of the specimen geometry (at least over a reasonable range), whereas the residual stress arises as a response to the actual geometry of the component. Hence, the residual stress in a range of different geometries and for a range of peened areas (in a given material) can be derived from the knowledge of a single eigenstrain depth profile, related to a particular set of peening parameters.

6. Construction of the full residual stress field from measured residual strains

As stated previously, determination of the full residual stress field (that satisfies overall equilibrium, compatibility and the boundary conditions), based on measured residual elastic strains at a finite number of measurement locations is a very demanding task. The eigenstrain technique offers a mean of dealing with this difficulty and the development of an inverse eigenstrain method to determine the full residual stress field is discussed below. A knowledge of the general form of the eigenstrain distribution produced by the LSP process is an essential prerequisite in this analysis. This allows a sensible choice of a parametric form for the experimental eigenstrain distribution (e.g. a polynomial distribution over a given depth). By combining this with residual strains measured at a finite number of locations, it is possible to determine a representative eigenstrain distribution (e.g. by matching the experimental results in a least squares sense). This may then be used to predict the residual stress state in the whole sample in the usual way. The advantage of this approach is that the elastic response of the workpiece to the eigenstrain will satisfy equilibrium, compatibility and the boundary conditions, so that the residual stress field produced is entirely self-consistent.

The least squares analysis requires the choice of a suitable parametric form for the eigenstrain distribution. Methods based on Chebyshev polynomials [17] are widely used in numerical analysis of least squares fits and they will be adopted here, although alternative choices are possible. We assume that the eigenstrain distribution ($\varepsilon^p(z)$) may be represented as a Chebyshev series of N polynomials (Eq. 1). The choice of N is too some extent arbitrary although it should be less than total number of strain measurements. Similarly, it should be large enough to capture the expected form of the eigenstrain distribution with acceptable accuracy. In practice the analysis can be carried out for a number of different N values and a check will be carried out to ensure that the results are largely independent of the value chosen.

All three principal components of the eigenstrain are required in the analysis [1]. However, as shown by Achintha and Nowell [1], it is only necessary to evaluate one component, since the other two may be determined by applying considerations of symmetry and of volume conservation in plastic deformation. It is also necessary to choose the depth of the eigenstrain distribution, a value little larger than the expected depth, indicated by FWHM measurements may be used. As long as this choice is sensible, the answer is largely independent of the choice. A typical example of this 'inverse eigenstrain' analysis will be discussed below.

In the example, Chebyshev polynomials of the first kind ($T_i(z)$; i = 0,1,2,3,..*N-1*) [17] are used and the coefficients c_i (Eq. 1) are unknown at the beginning of the analysis. The first step involves implementing each $T_i(z)$ as an eigenstrain distribution in separate FE models and determining the respective residual strain distributions ($\varepsilon_i(z)$) in the specimen. The response of the specimen to the installed eigenstrains is elastic, and hence the resultant residual strain distribution ($\varepsilon_e(z)$) caused by the original eigenstrain distribution is determined as the sum of that caused by each polynomial $\varepsilon_i(z)$ multiplied by the coefficients c_i (Eq. 2). Finally, the coefficients c_i (i=0,1,2,3,..*N-1*) are determined by matching $\varepsilon_e(z)$ with measured residual strains in a least squares sense. Details of a comprehensive least squares analysis of an inverse eigenstrain analysis can be found in Korsunsky [18] and will not therefore be repeated here.

Once an appropriate estimate for the eigenstrain distribution has been established, the complete residual stress distribution can be determined through a single static FE model in the usual way. The flowchart given in Fig. 13 shows the step-by-step procedure of this analysis.

$$\varepsilon_p^i(z) = \sum_{i=0}^{N-1} C_i T_i(z) \qquad [1]$$

$$\varepsilon_e(z) = \sum_{i=0}^{N-1} C_i \varepsilon_i(z) \qquad [2]$$

Figure 14 shows the results of a simple test case, where the measured strains (ε_{xx}^{p}) are shown as symbols. The specimen is 10 mm thick and the residual strain measurements within 4.5 mm into the sample were considered. The depth of the eigenstrain distribution and the number of Chebyshev polynomials (*N*) used in the analysis are determined such that the results are largely independent of the chosen values. The FWHM measurements indicated that the depth of the eigenstrain distribution presents in the specimen is about 3.3 mm deep. This depth was first chosen and the inverse analysis was carried out for selected eigenstrain distributions chosen using Chebyshev series of 9, 11 and 13 polynomials; the results are shown in Fig. 14. Results show that the eigenstrain distribution and the residual elastic strains predicted by the analyses for all these cases are almost identical. A small difference between the values predicted by the analysis with *N*=9 and those predicted by the analyses with *N*= 11 and 13 can be seen at the depth range 2.7–3.3 mm. As it can be seen from Fig. 14b, this depth is approximately the location where the tensile stress starts to drop from its peak value. As expected, a Chebyshev series with a large number of polynomials is required to appropriately capture a variation of this nature. Results suggest that the choice of *N*=13 is capable of accurately reconstructing full stress field present in the specimen. The subsequent inverse eigenstrain analyses discussed below are based on Chebyshev series of 13 polynomials.

In the earlier analysis the depth of the eigenstrain distribution was chosen to equal that indicated by FWHM results. Here we will show that accurate results can still be obtained with a sensible but arbitrary choice for the depth of the eigenstrain in cases where the corresponding FWHM data is unavailable. Fig. 15 shows the results from the analyses of the same specimen after selecting the depth of the eigenstrain distribution to be 2.8, 3.3, 3.8 and 4.3 mm respectively. These values were chosen to study sensitivity of the results if the chosen depths were slightly lower and higher than the actual depth (3.3 mm) indicated by FWHM measurements. Fig. 15a shows that the eigenstrain distribution predicted by the

analyses based on respective chosen depths are almost identical within the depth range 0.0–2.5 mm. As expected, the tail region of the predicted eigenstrain distribution is slightly influenced by the choice. In particular, a notable difference can be seen when the eigenstrain was forced to reach zero at a depth of 2.8 mm. However, the residual strain (or stress) distribution predicted by the analyses are largely unaffected by the selected eigenstrain depth (Fig. 15b). In particular, the predicted results for the material close to the surface (i.e. depths up to about 2.5 mm) are almost independent of the chosen eigenstrain depth and this is usually the region of most concern in design.

Conclusions

The paper has presented numerical modelling results concerning the residual stress field associated with laser shock peening (LSP) applied to flat large Ti-6Al-4V specimens. The study has shown that the hybrid explicit/eigenstrain finite element modelling approach works extremely well. Eigenstrain distributions inferred from an explicit FE simulation of a representative small array of LSP shots can be used to accurately model the residual stress generated by arrays of 100%, 200% and 300% peen cases where the use of a completely explicit analysis may be impractical.

The results show that the eigenstrain caused by a 3 x 3 mm LSP shot in an wider patch of surface treatment is substantially limited to the immediately below it and is not significantly affected by the eigenstrain present in the surrounding area. Thus, neglecting relatively minor edge effects, it is appropriate to model the eigenstrain due to an array of pulses in a single layer as that due to a single pulse, but applied over the correct area.

The results of subsequent layers of LSP arrays with offsets 50% and 0% respectively show that the eigenstrain depth profile due to multiple layers of pulses is not significantly affected

by the area of the array or the degree of offset between the subsequent layers. Thus, the residual stress can be determined from a static FE model by incorporating the eigenstrain depth profile obtained from a representative simple array with an assumed convenient offset between the subsequent layers of LSP.

The model predictions for the eigenstrain distributions generated by LSP compare well with experimental measurements of plastic strain obtained from a neutron diffraction technique and this provides a useful validation of the approach.

Finally, the eigenstrain technique may be used to construct the full residual stress field in a component that satisfies equilibrium and compatibility conditions of the specific problem, based on measured residual elastic strains at a finite number of measurement locations. Irrespective of whether the eigenstrain distribution is obtained from experimental measurements in this manner, or from explicit FE analysis, it may be used in further calculations. For example,

once the eigenstrain corresponding to a particular LSP treatment is known, the residual stress in new geometries and/or during subsequent loading can be calculated in a computationally efficient manner. Results from calculations of this nature will be published elsewhere.

Acknowledgements

The financial support of the Engineering and Physical Sciences Research Council (EPSRC) and the UK Ministry of Defence under grant numbers EP/F026226/1 and EP/F026730/1 is gratefully acknowledged. The authors would like to thank Dr Alexander Evans for his help

in obtaining beam time and in undertaking experiments at the Institute Laue Langevin, Grenoble.

References

[1] M. Achintha, D. Nowell, Eigenstrain modelling of residual stresses generated by laser shock peening. *Journal of Material Processing Technology*, 211(6), 2011, 1091-1101.

[2] A. King, A. Steuwer, Woodward C, Withers P.J. Effects of fatigue and fretting residual stress introduced by laser shock peening. *Materials Science and Engineering:A*, 435-436(5), 2006, 12-18.

[3] K.Ding, L. Ye, 2006. *Laser shock peening: Performance and process simulation*, Woodhead, Cambridge, UK.

[4] J. D. Eshelby, The Determination of the Elastic Field of an Ellipsoidal Inclusion and Related Problems. Proc. Roy. Soc. London, Ser. A, 1957. 241: p. 376-396.

[5] A. M. Korsunsky, G. M. Regino, D. Nowell, Variational eigenstrain analysis of residual stresses in a welded plate. *International Journal Solids and Structures*, 44(13), 2006, 4574-4591.

[6] Prime, M. B., Hill, M.R. Measurement of fibre-scale residual stress variation in a metal-matrix composite. *Journal of Composite Materials*, 38(23), 2004, 2079-2095.

[7] A. M. Korsunsky, Residual elastic strains in autofrettaged tubes: elastic-ideally plastic model analysis. *Journal of Engineering Materials and Technology*, 129(1), 2007, 77-81.

[8] A. T. DeWal, M. R. Hill, Eigenstrain-based model for prediction of laser peening residual stresses in arbitrary three-dimensional bodies. Part 1: model description. *Journal of Strain Analysis*, 44(1), 2009, 1-11.

[9] McGeachie, I., 2010. Private communication, Metal Improvement Company, Earby, UK.

[10] H. K. Amarchinta, R. V. Grandhi, K. Langer, D. Stargel, Material model validation for laser shock peening. *Modelling and Simulation in Material Science and Engineering*. 17(1), 2009, 1-15.

[11] LS-DYNA (V971) - Livermore Software Technology Corporation (LSTC)

[12] Abaqus 6.10 - SIMULIA

[13] J. E. Masse, G. Barreau, Laser generation of stress waves in metal. *Surface and Coating Technology*, 70(2/3), 1995, 231-234.

[14] J. Y. Kim, I. O. Shim, H. K. Kim, S. S .Hong, S. H. Hong, Dynamic deformation and high velocity impact behaviours of Ti-6Al-4V Alloys. *Materials science Forum*, 2007, 2269-2274.

[15] R. D. Haigh, M.T. Hutchings, J. A. James, S. Ganguly, R. Mizuno, K. Ogawa, S. Okido, A.M. Paradowska, M.E. Fitzpatrick, Neutron diffraction residual stress measurements on girth-welded 304 stainless steel pipes with weld metal deposited up to half and full pipe wall thickness. *International Journal of Pressure Vessels and Piping*, 2012, 1-11.

[16] C. Ye, G. J. Cheng, laser shock peening of nanoparticles integrated alloys: Numerical simulation and experiments. *Journal of Manufacturing Science and Engineering*, 132(6), 2010.

[17] J.C. Mason, D.C. Handscomb Chebyshev polynomials. Boca Raton, FL: Chapman & Hall/CRC, 2003.

[18] A. M. Korsunsky, Eigenstrain analysis of residual strains and stresses. *Journal of Strain Analysis for Engineering Design*, 44(1), 2009, 29-43.

Suggested changes by the Reviewer #4 were made in the figures (the corrected figures; Figs. 1, 4, 5, 6, 11, 14; uploaded with the revised manuscript)

List of figures

Fig. 1. Step-by-step procedure of an eigenstrain analysis of the LSP process

Fig. 2. Geometry of the workpiece

Fig. 3. (a) A substantially uniform surface indent suggests that the effect of a drop in pressure towards the edges of the pulse is minor (half the pulse area is shown)

(b) A simplified pressure–time history of the dynamic load used to represent the effect of pressure pulse in the explicit FE simulations

Fig. 4. (a) Typical results, showing that the stabilised plastic strain is approximately uniform with *x* and *y*, over the area covered by the pulse

(b) Variation of eigenstrain along the lateral direction (a new figure)

(c) Polynomial representation of eigenstrain component ε_{xx}^{p} at the centre (0, 0, *z*) of the pulse

Fig. 5. (a) Stabilised plastic strain in the specimen viewed over the half plane y=0

(b) Variation of ε_{xx}^{p} with *z* at three different locations (A, B, C marked in (a)) in the array

Fig. 6. (a) In-plane stress component, σ_{yy}, generated by the array of LSP shots

(b) Comparison between in-plane residual stresses generated along (0, 0, *z*) by the array and by an single LSP shot

Fig. 7. (a) Two layers of peening with the shots in the second layer 50% offset relative to the those of the initial layer in both directions *x* and *y*

(b) A simple array with just one pulse overlaid at 50% offset to four shots in layer one

(c) Stabilised plastic strain obtained from explicit FE model before and after the fifth pulse

Fig. 8. Eigenstrain distributions obtained from explicit FE models for multiple layers of LSP shots as described in Sections 3, 4.1 and 4.2

Fig. 9. (a) An array of three LSP shots, where the last two shots were arranged to give 50% overlap with the first shot in the *x* and *y* directions

(b) Stabilised plastic strain on the surface ($z = 0$) after each LSP shot

Fig. 10. Eigenstrain distribution is not affected by the degree of overlap between the adjacent shots in the subsequent layers

Fig. 11. (a) Measured increase in neutron diffraction peak broadening (FWHM) with depth at the centre of the peen area for a 200% peened specimen (I = 9 GW/cm^2)

(b) Comparison between the predicted eigenstrain ε_{xx}^{p} and increase in FWHM relative to the parent value for 200% peen using different laser intensities (I = 9, 6 and 3 GW/cm^2 respectively)

(c) Relationship between ΔFWHM and ε_{xx}^{p}

Fig. 12. Variation of in-plane residual stress (σ_{yy}) with depth z under multiple layers of LSP shots (for single and arrays of LSP shots)

Fig. 13. Step-by-step procedure of an inverse eigenstrain analysis of the LSP process

Fig. 14. (a) Inferred eigenstrain distribution that best described the measured residual strain results (symbols in (b))

(b) Reconstructed residual elastic strain distribution; from analyses based on different values for total number of Chebyshev polynomials used

Fig. 15. Results from inverse eigenstrain analyses for: (a) estimate of eigenstrain distribution (b) reconstructed residual elastic strain distribution; from analyses based on different values for the depth of the eigenstrain distribution

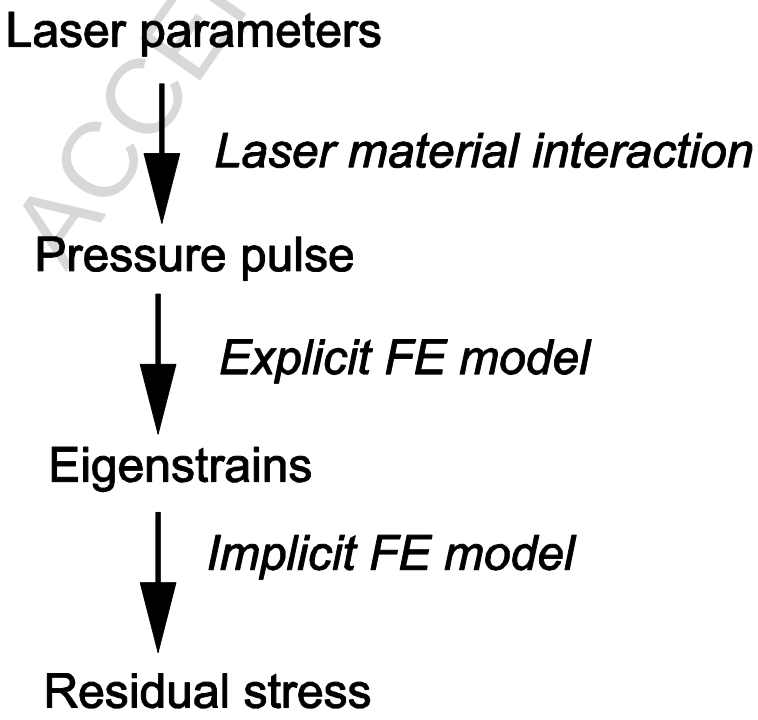

Fig. 1

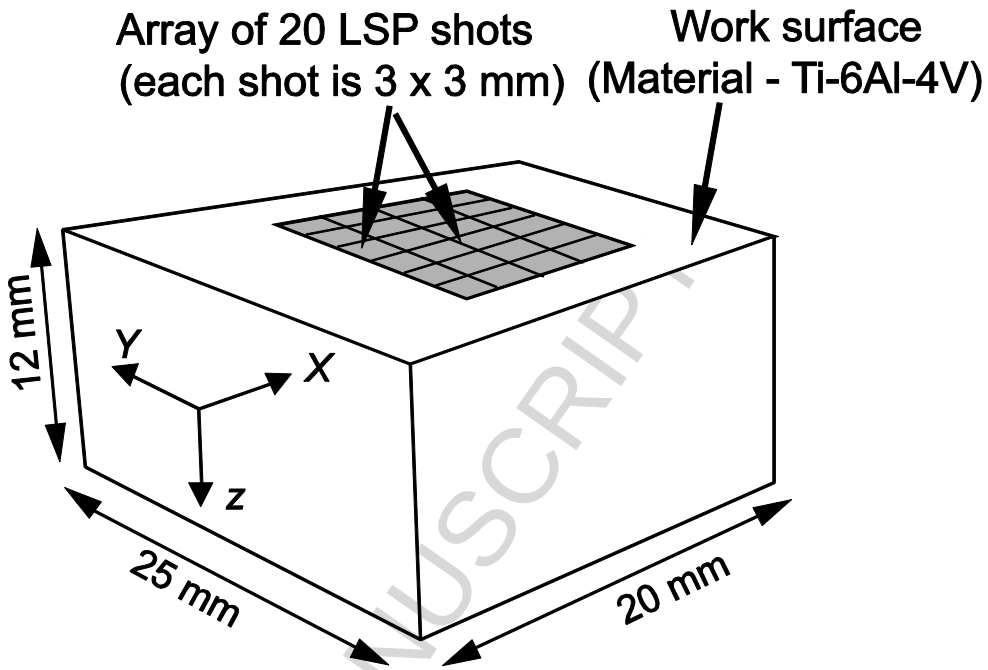

Fig. 2

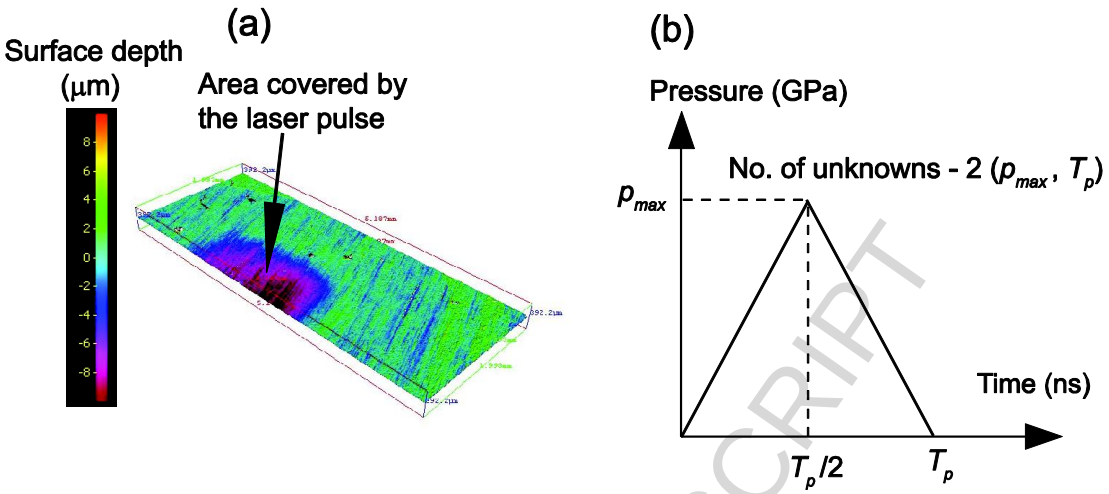

Fig. 3

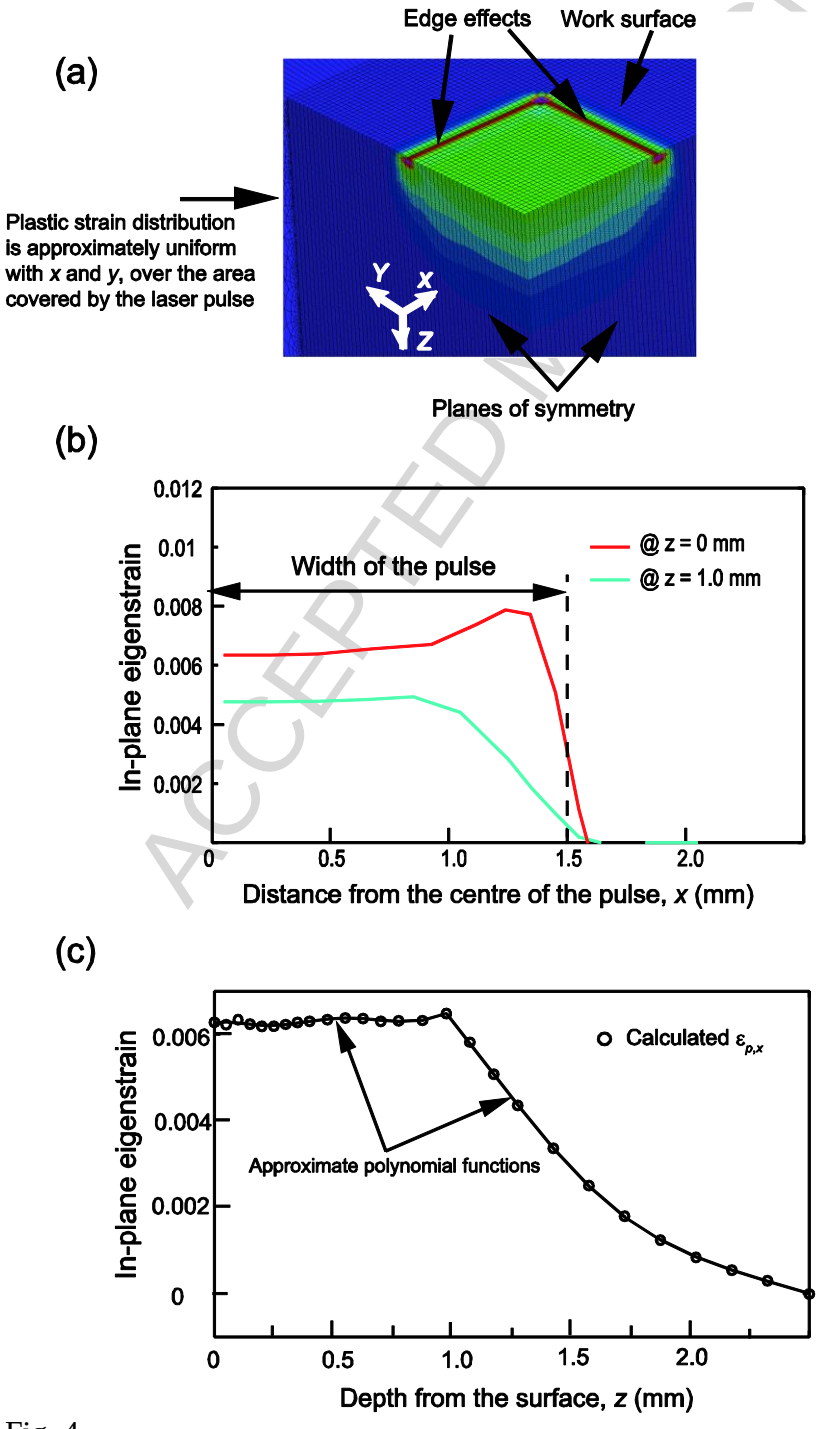

Fig. 4

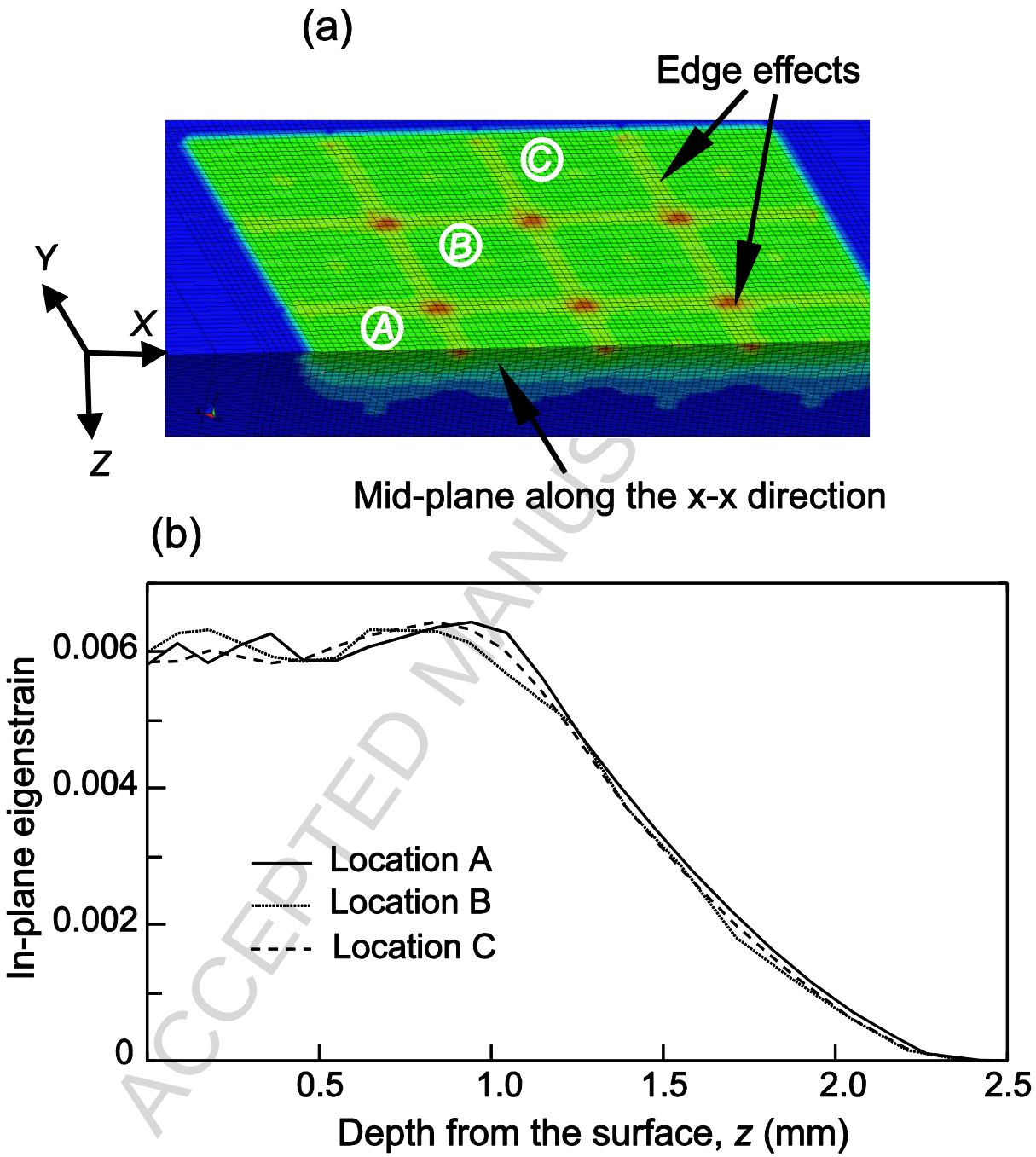

Fig. 5

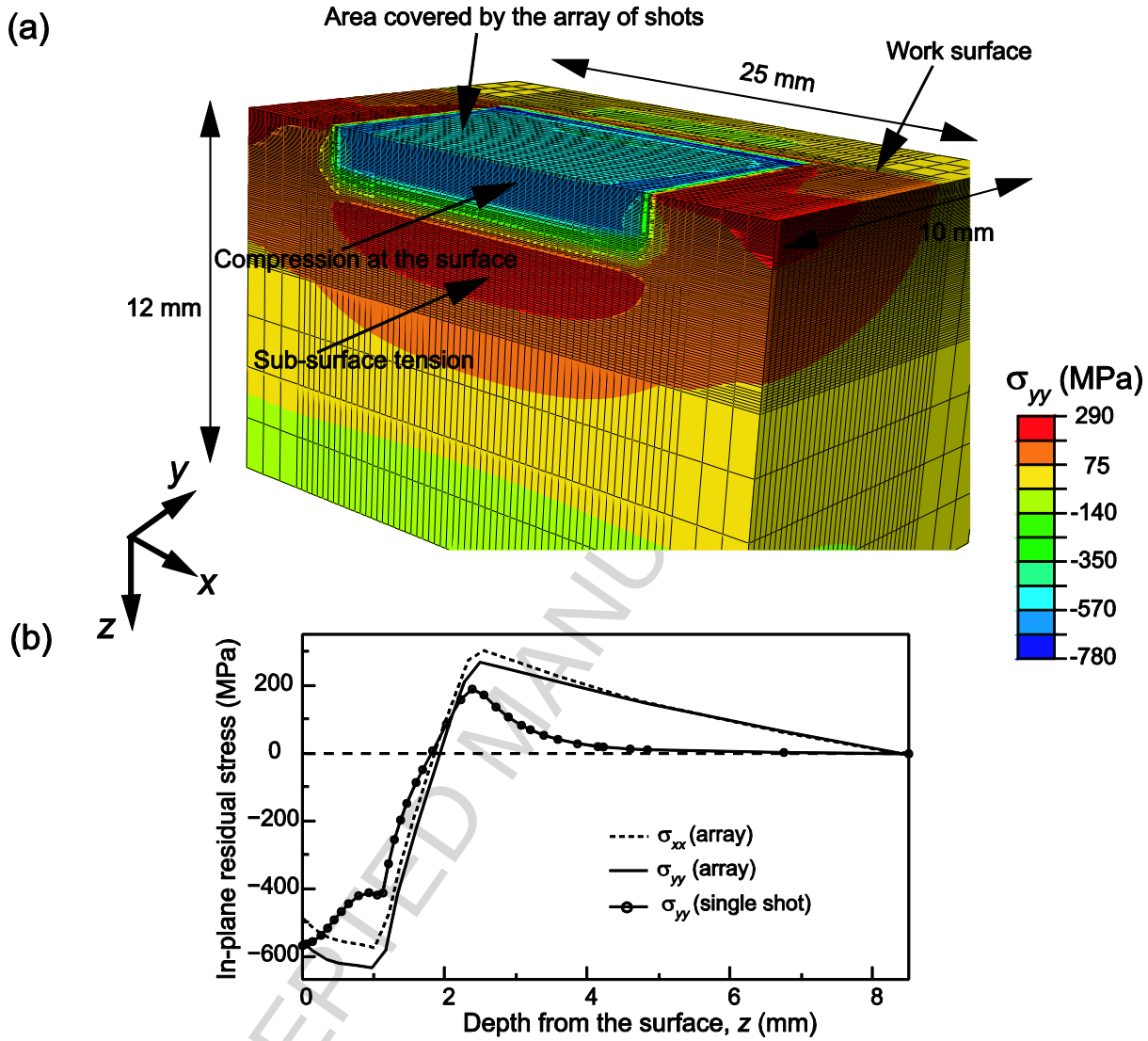

Fig. 6

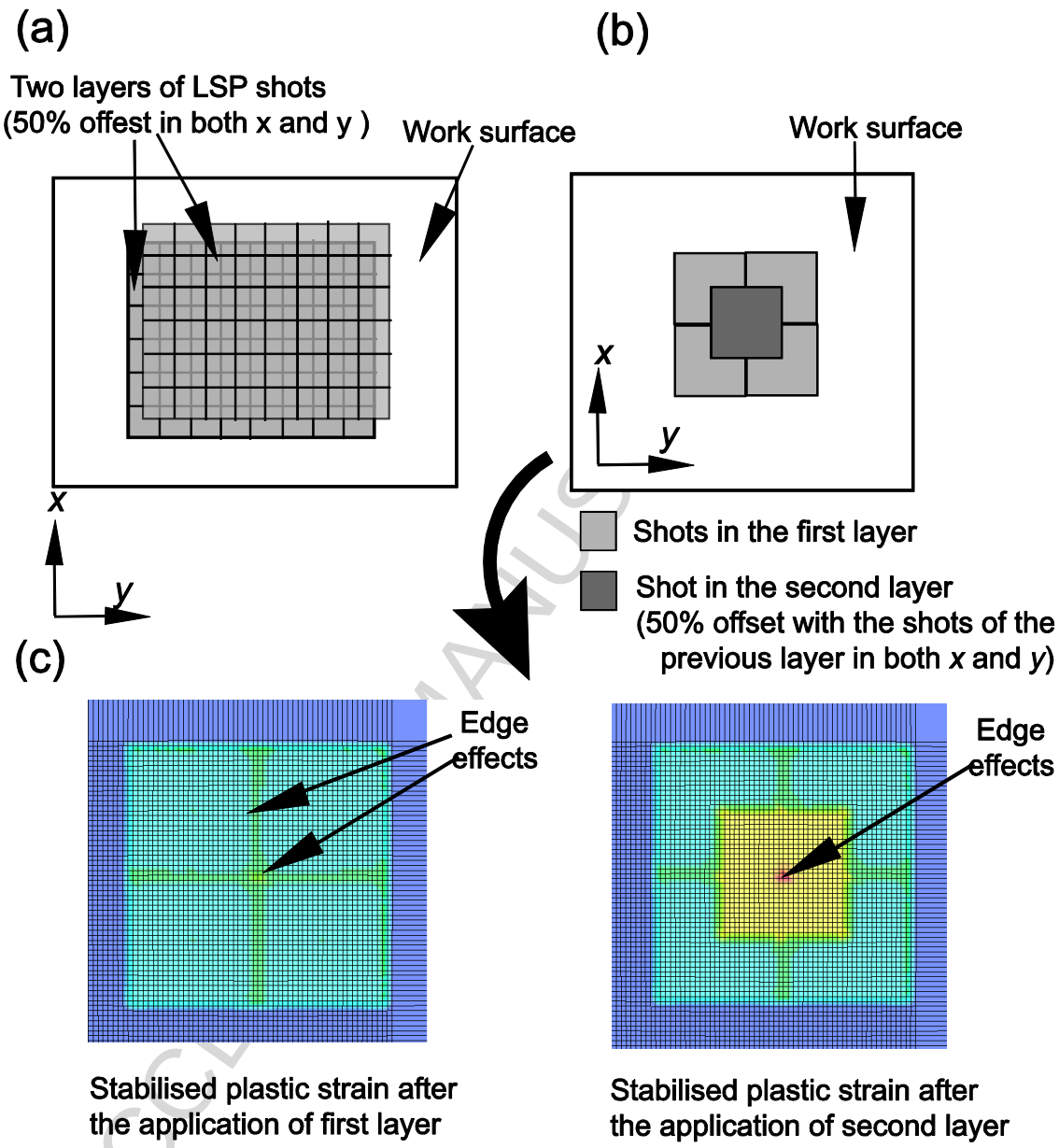

Fig. 7

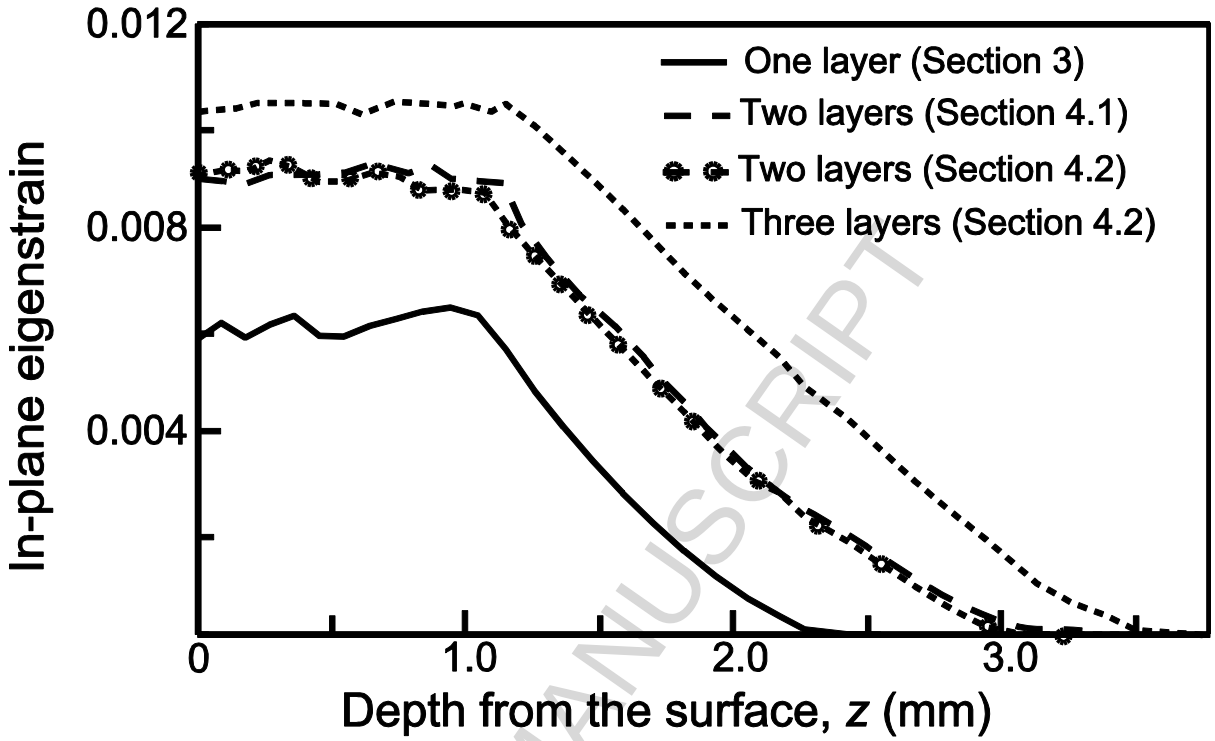

Fig. 8

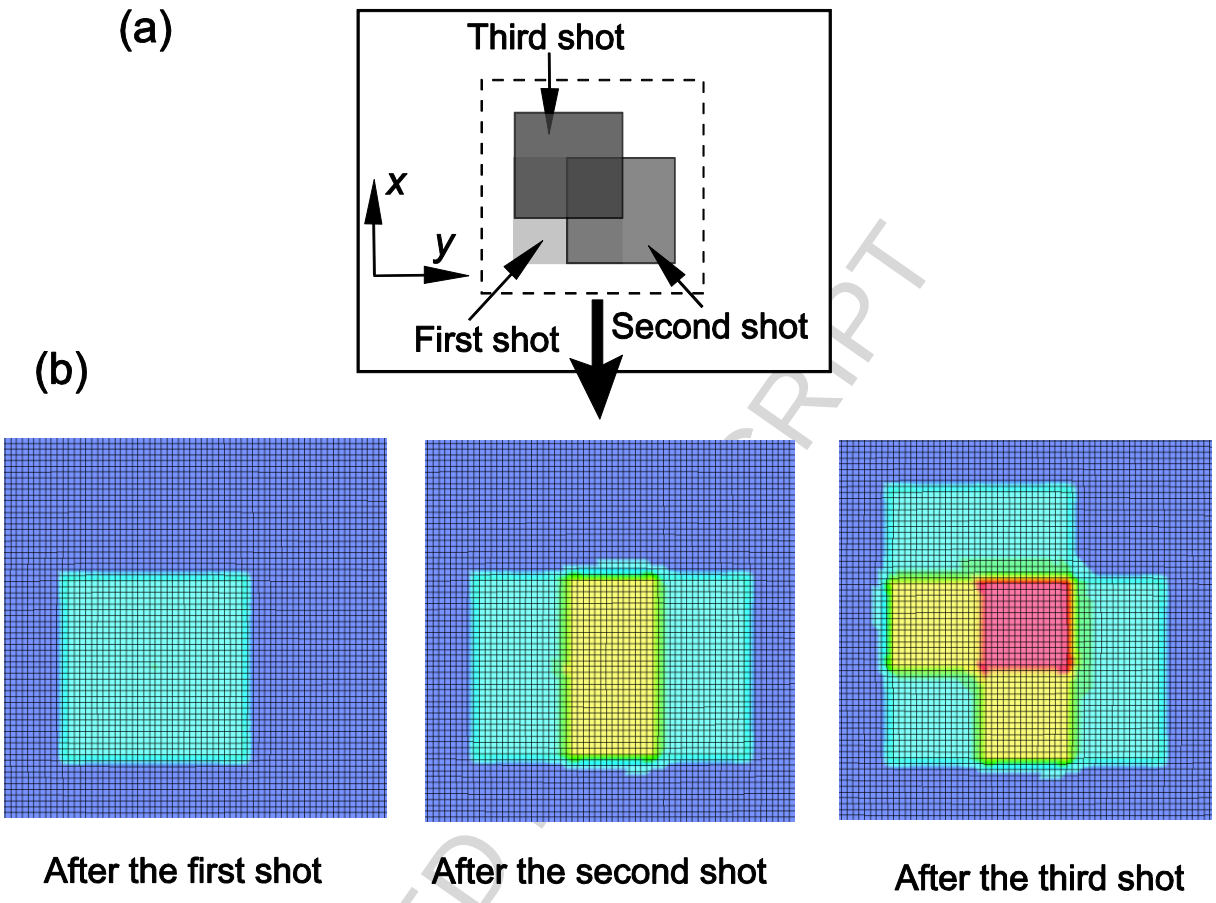

Fig. 9

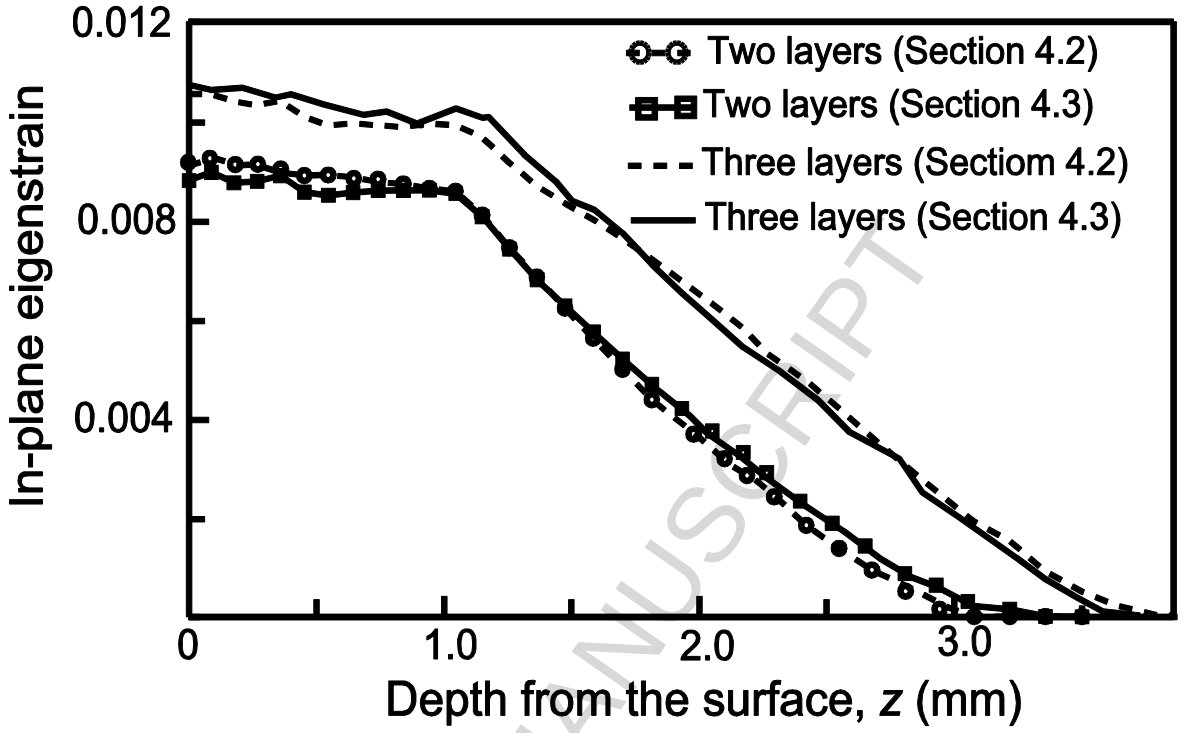

Fig. 10

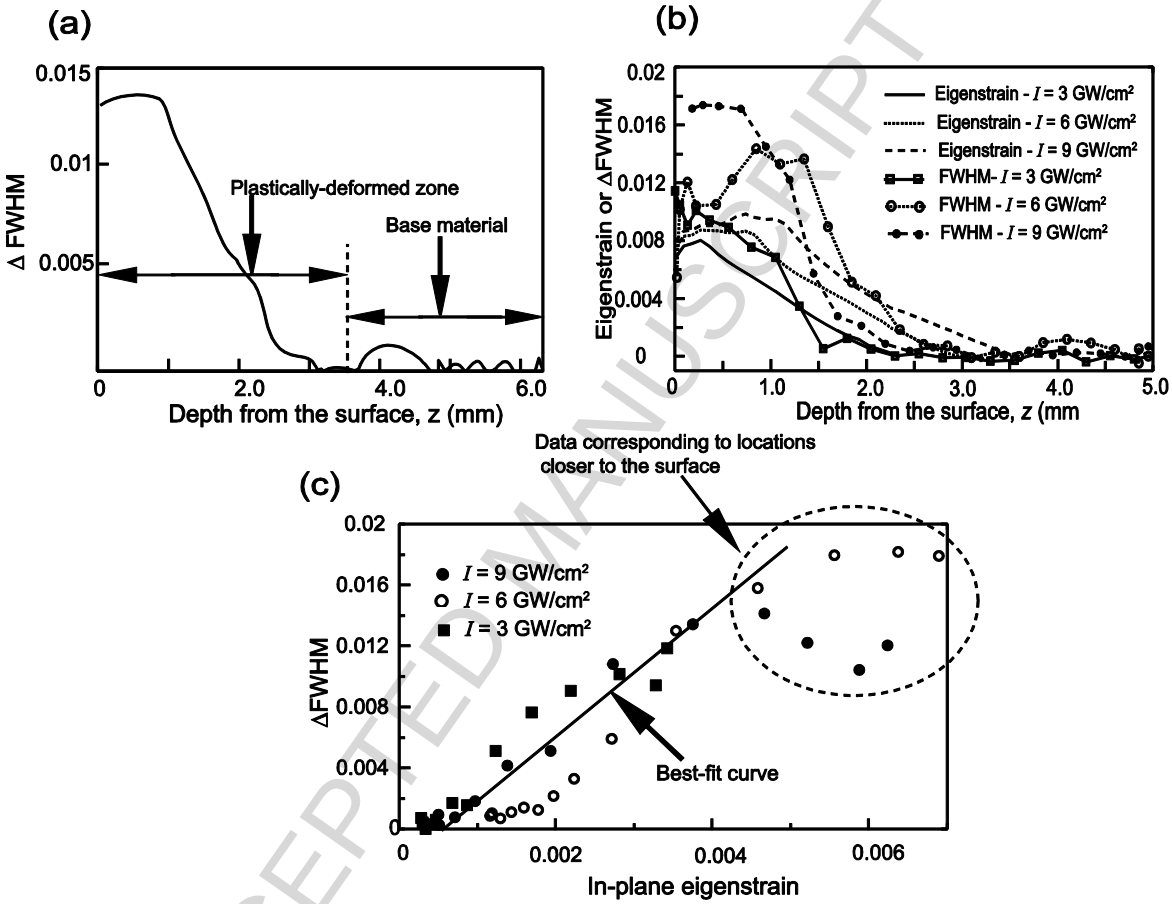

Fig. 11

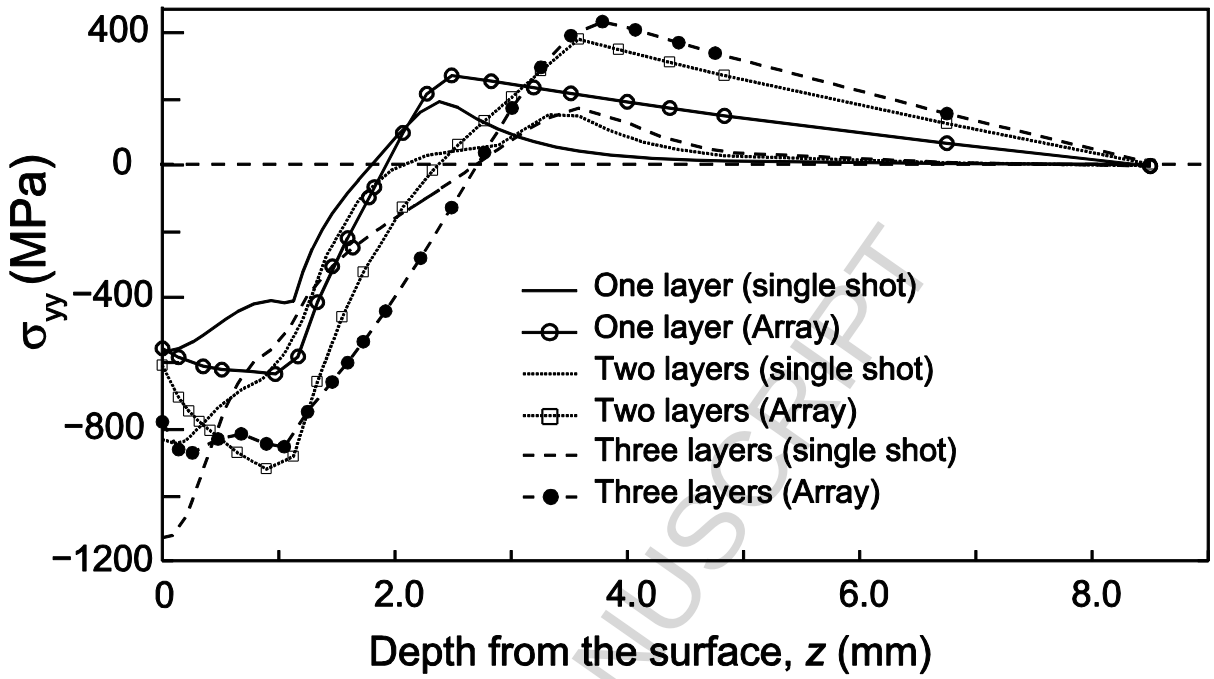

Fig. 12

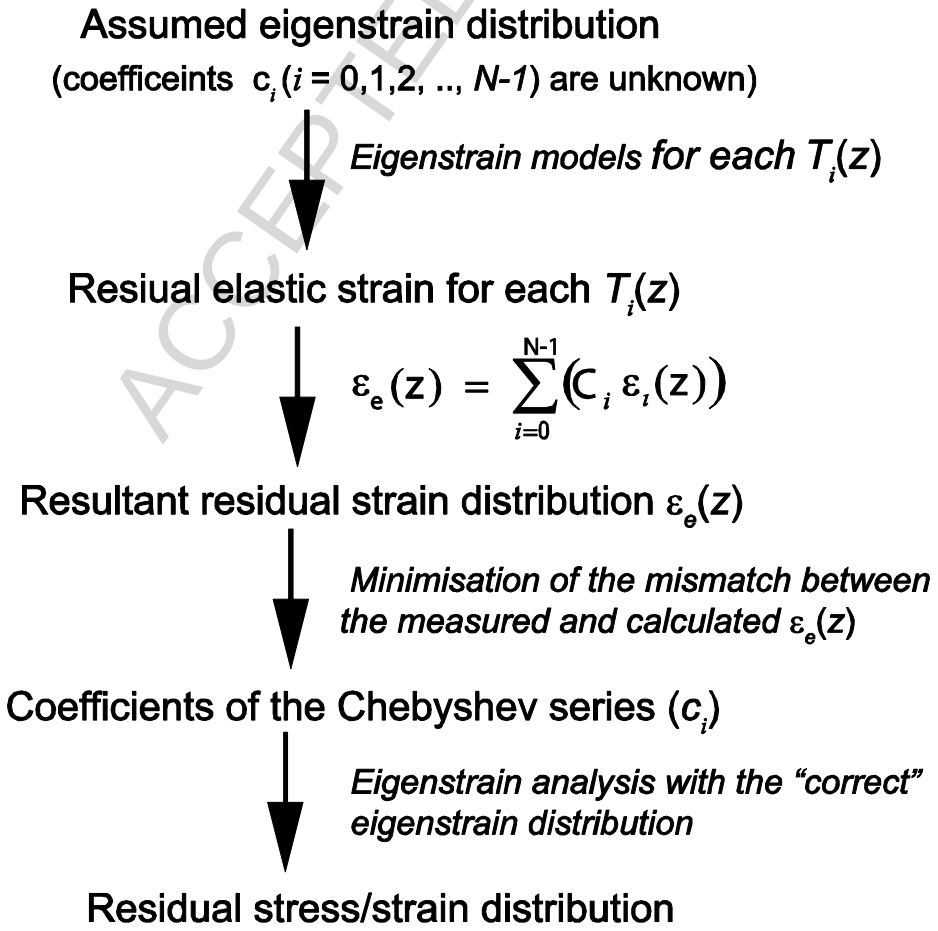

Fig. 13

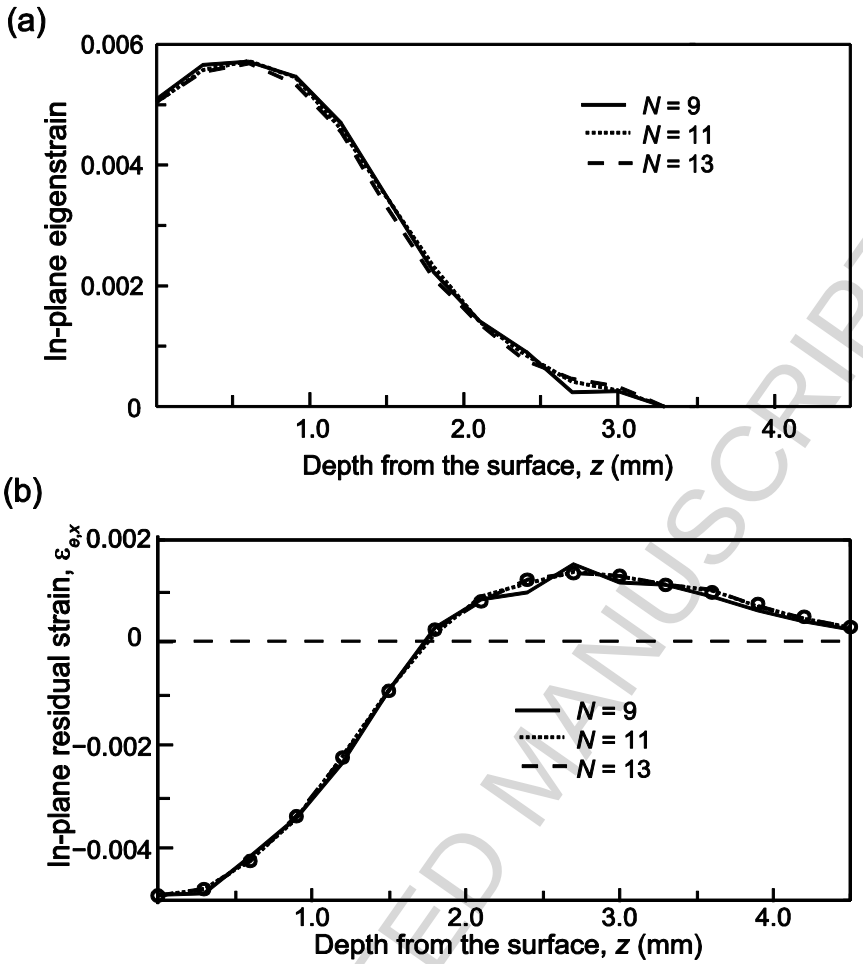

Fig. 14

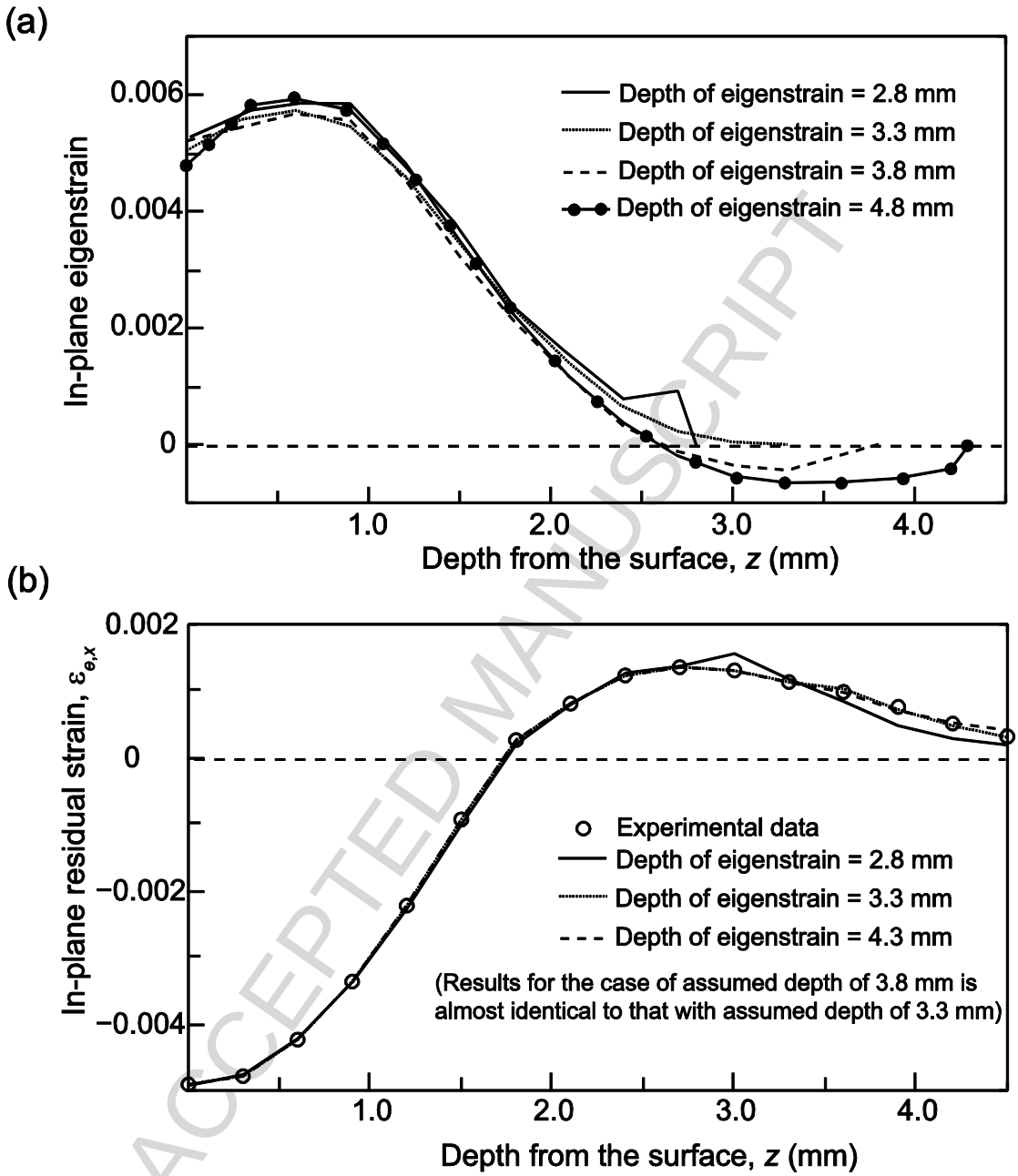

Fig. 15

Highlights

- Eigenstrain approach works well to model the process of laser shock peening
- Eigenstrain depth profile can be obtained from an analysis of a simple array
- Full residual stress field can be determined from inverse eigenstrain analysis